

DOCTORAL THESIS

**IMPROVEMENT IN PERFORMANCES OF DYE-SENSITIZED SOLAR
CELL BASED ON NANOSTRUCTURED RUTILE-PHASED TiO₂**

MOHD KHAIRUL BIN AHMAD

Graduate School of Science and Technology

Department of Optoelectronics and Nanostructure Science

Shizuoka University

Japan

June 2012

Abstract

Renewable energy has been extensively studied nowadays by many researchers around the world. Among this renewable energy, there is solar cell which is one of the promising candidates to overcome the energy crisis in the future. With low cost production and simple fabrication of Dye-sensitized solar cell (DSC), DSC is one of the best solar cell which could overcome the energy problem in the future. Anatase-phased TiO_2 film is the conventional material for photoelectrode semiconductor layer of the DSC, even though rutile-phased TiO_2 gives same characteristics such as band gap property. It may be due to the preparation condition for the rutile phase, which needs higher temperature than $900\text{ }^\circ\text{C}$ for preparation. The rutile-phased TiO_2 has good electron transportation compared to the anatase phase. Because of this, the rutile-phased TiO_2 has been applied to some electronic devices.

Nanostructures play main roles in electron transportation in any electronic devices. By preparing the rutile-phased TiO_2 and applying nanostructures in the fabrication, DSC performances should be improved. The rutile-phased TiO_2 , therefore, is also strong candidate for high performance DSCs.

In the present study, DSCs based on the rutile-phased TiO_2 have been successfully prepared and their performances have been improved by applying two kinds of nanostructures; aligned rutile-phased TiO_2 nanorods and rutile-phased TiO_2 nanoflowers. Both nanostructures were prepared using hydrothermal method at $150\text{ }^\circ\text{C}$ for different reaction times. The nanostructures were grown directly on a fluorine doped tin oxide glass (FTO coated glass). As for the growth mechanism, the aligned rutile-phased TiO_2 nanorods were firstly grown on the FTO coated glass. Then, through chemical reaction and pressure inside an autoclave, the rutile-phased TiO_2 nanoflowers were synthesized and deposited on top of the aligned nanorods. Mixture of titanium butoxide, hydrochloric acid, cetyltrimethylammonium bromide

(CTAB) and deionized water was prepared and put into the 300 ml autoclave made by Teflon. The FTO plates were put in horizontally with FTO surface facing upwards. After the hydrothermal process, the plates were rinsed with deionized water and annealed at 450 °C for 30 min.

Field emission scanning electron microscopy (FE-SEM) was carried out to observe a surface morphology and a thickness of the prepared rutile-phased TiO₂ films. X-ray diffractions (XRD) characterization was taken to examine and determine the TiO₂ crystalline phases in prepared films. Solar simulator was used to measure the performances of Dye-sensitized solar cell based on the rutile-phased TiO₂. For the dye adsorption property, UV-Vis-NIR spectrophotometer measure an amount of dye adsorption in the film. Electrochemical Impedance Spectroscopy (EIS) was also used to determine a conductivity of the DSCs.

In early stage of the study, influence of TBOT concentration on the surface morphology, structural properties and solar cell efficiency were investigated for the rutile-phased TiO₂ films and the DSCs based on the films. The highest energy conversion efficiency, 0.4 % was achieved using different solution concentration for the preparation under the solar light illumination 100 mWcm⁻² (1.5 AM). Low dye adsorption in the film was the reason for low energy conversion efficiency.

By growing the rutile-phased TiO₂ nanoflowers on top of the aligned TiO₂ nanorods, the dye adsorption is increased. This is due to an increase in surface area of TiO₂ layer for dye to adsorb. Cetyltrimethylammonium bromide (CTAB) is introduced to control and enhance the growth of rutile-phased TiO₂ nanoflowers. As a result, the best efficiency of 3.11 % is obtained and the improvement is mainly attributed to an introduction of TiO₂ nanoflowers for more dye adsorption.

Energy conversion efficiency as high as 4.27 % is achieved through some improvement on the DSC based on rutile-phased TiO₂ layer. Two steps of hydrothermal process are conducted. First step is to prepare only the aligned rutile-phased TiO₂ nanorods. At this step, very dense and aligned nanorods are obtained with 3 μm in length. In the second step, the rutile-phased TiO₂ nanoflowers are synthesized. By preparing new solution with some modification, a large amount of TiO₂ nanoflowers with smaller sizes are obtained. The thickness is about 15 μm. Energy conversion efficiency of 4.27 % for nanostructured rutile-phased TiO₂ based DSC is the highest record nowadays.

TABLE OF CONTENTS

THE TITLE	i
ABSTRACT	ii
ACKNOWLEDGEMENT	v
OUTLINE OF THESIS	vii
TABLE OF CONTENTS	vii
LIST OF TABLES	xi
LIST OF FIGURES	xii
LIST OF ABBREVIATIONS	xiv
CHAPTER 1	
INTRODUCTION AND BACKGROUND OF RESEARCH	
1.1 Introduction	1
1.2 Solar cell history	
1.2.1 Early stage of solar cell	1
1.2.2 Middle stage of solar cell	3
1.2.3 Current stage of solar cell	3
1.3 Structure of dye-sensitized solar cell (DSC)	4
1.4 Hydrothermal method	
1.4.1 History and definition of hydrothermal method	8
1.5 Background research	
1.5.1 Dye-sensitized solar cell	9
1.5.2 Advantages of one dimensional nanostructured rutile-phased TiO ₂ towards DSC	10
1.5.3 Rutile-based dye-sensitized solar cell and its advantages	11
1.6 Thesis objectives	12
1.7 References	13

CHAPTER 2

GROWTH AND APPLICATION OF TiO₂ NANORODS IN DSC USING HYDROTHERMAL METHOD

2.1	Introduction	16
2.2	Experimental	16
2.3	Results and discussion	
	2.3.1 Surface morphology	18
	2.3.2 Structural property	20
	2.3.3 Photovoltaic properties	21
2.4	Conclusion	23
2.5	References	24

CHAPTER 3

IMPROVEMENT IN PHOTOVOLTAIC PERFORMANCE OF RUTILE-PHASED TiO₂ NANORODS BASED DYE-SENSITIZED SOLAR CELL (DSC)

3.1	Introduction	25
3.2	Experimental	
	3.2.1 Preparation of rutile-phased TiO ₂ nanorods photoelectrodes	26
	3.2.2 Preparation of dye-sensitized solar cell (DSC)	27
3.3	Characterization	29
3.4	Results and discussion	
	3.4.1 Surface morphology and structural property: r-TNRs/r-TNFs preparation at various reaction times	30
	3.4.2 Surface morphology and structural property: r-TNRs/r-TNFs preparation at various reaction times with CTAB	32
	3.4.3 Effect of CTAB surfactant in hydrothermal process	35
	3.4.4 Electrochemical impedance spectroscopy (EIS)	42
3.5	Conclusion	45
3.6	References	46

CHAPTER 4

HYDROTHERMAL GROWTH OF BILAYERED RUTILE-PHASED TiO₂ NANORODS/NANOFLOWERS BASED PHOTOELECTRODE FOR HIGH PERFORMANCE DSC

4.1	Introduction	47
4.2	Experimental	48
4.3	Results and discussion	
	4.3.1 Structural property	50
	4.3.2 Surface morphology	51
	4.3.3 Photovoltaic properties	53
4.4	Conclusion	58
4.5	References	59

CHAPTER 5 SUMMARY, CONCLUSIONS AND FUTURE WORKS

5.1	Summary and conclusion	60
5.2	Future works	63
5.3	References	63

LIST OF PUBLICATIONS	64
-----------------------------	-----------

LIST OF TABLES

Table 2.1 Photovoltaic properties of DSC with different TBOT concentrations

Table 3.1 Photovoltaic properties derived from Figure 3.11 and the amount of dye adsorption

Table 3.2 Photovoltaic properties derived from Figure 3.12 and the amount of dye adsorption

Table 4.1 Photovoltaic properties derived from Figure 4.4 and those for the DSC based on anatase-phased TiO_2 photoelectrode

LIST OF FIGURES

- Figure 1.1 Configuration of conventional Dye-sensitized Solar Cell (DSC)
- Figure 1.2 Principle operation of Dye-Sensitized Solar Cell (DSC)
- Figure 2.1 (a) the surface morphology of nanostructured TiO₂ film synthesized at 150°C with 0.5 ml of TiO₂ precursor and (b) its cross section
- Figure 2.2 (a) the surface morphology of nanostructured TiO₂ film synthesized at 150°C with 0.7 ml of TiO₂ precursor and (b) its cross section
- Figure 2.3 (a) the surface morphology of nanostructured TiO₂ film synthesized at 150°C with 1.0 ml of TiO₂ precursor and (b) its cross section
- Figure 2.4 XRD profiles of TNRs film with different TBOT concentrations; (a) 0.5ml, (b) 0.7ml and (c) 1.0ml
- Figure 2.5 I-V characteristics of DSC based on the TNRs films with different TBOT concentrations
- Figure 3.1 Schematic diagram of the dye-sensitized solar cell based on a combination of rutile-phased TiO₂ nanoflower (r-TNF) with rutile-phased TiO₂ nanorods (r-TNR) formed on the FTO glass
- Figure 3.2 (a-1) surface morphology of nanostructured TiO₂ film synthesized at 150°C for 2 h, and (a-2) its cross sections
- Figure 3.3 (a-1) surface morphology of nanostructured TiO₂ film synthesized at 150°C for 5 h, and (a-2) its cross sections
- Figure 3.4 (a-1) surface morphology of nanostructured TiO₂ film synthesized at 150°C for 10 h, and (a-2) its cross sections
- Figure 3.5 (a-1) surface morphology of nanostructured TiO₂ film synthesized with CTAB at 150°C for 2 h, and (a-2) its cross sections
- Figure 3.6 (a-1) surface morphology of nanostructured TiO₂ film synthesized with CTAB at 150°C for 5 h, and (a-2) its cross sections
- Figure 3.7 (a-1) surface morphology of nanostructured TiO₂ film synthesized with CTAB at 150°C for 10 h, and (a-2) its cross sections

- Figure 3.8 XRD profiles of the rutile-phased nanostructured TiO₂ films synthesized at 150°C for 2 h, 5 h and 10 h
- Figure 3.9 (a-1) surface morphology of the nanostructured TiO₂ film synthesized at 150°C for 2 h without CTAB, and (a-2) its cross section
- Figure 3.9 (b-1) surface morphology of the nanostructured TiO₂ film synthesized at 150°C for 2 h with the addition of CTAB, and (b-2) its cross section
- Figure 3.10 XRD diffraction profiles of the rutile-phased nanostructured TiO₂ films with CTAB, synthesized at 150°C for 2 h, 5 h and 10 h
- Figure 3.11 I-V characteristics of DSC based on the rutile-phased nanostructured TiO₂ film synthesized without CTAB at 150°C for 2 h, 5 h and 10 h
- Figure 3.12 I-V characteristics of DSC based on the rutile-phased nanostructured TiO₂ film synthesized with CTAB at 150°C for 2 h, 5 h and 10 h
- Figure 3.13 IPCE spectra of DSCs based on the rutile-phased nanostructured TiO₂ films synthesized with CTAB at 150°C for 2 h, 5 h and 10 h
- Figure 3.14 EIS spectra of DSCs based on the rutile-phased nanostructured TiO₂ films synthesized without CTAB at 150°C for 2 h, 5 h and 10 h
- Figure 3.15 EIS spectra of DSCs based on the rutile-phased nanostructured TiO₂ films synthesized with CTAB at 150°C for 2 h, 5 h and 10 h
- Figure 4.1 XRD patterns of the r-TNRs layer and the r-TNRs/r-TNFs bilayer
- Figure 4.2 SEM images of (a) the top view of aligned r-TNRs layer, (b) its cross-section, (c) top view of the r-TNRs/r-TNFs bilayer and (d) its cross-section
- Figure 4.3 IPCE spectra of the DSC fabricated using aligned r-TNRs layer, r-TNRs/r-TNFs bilayer and anatase-phased TiO₂ as photoelectrode
- Figure 4.4 Photocurrent-voltage characteristics of the DSC fabricated using aligned r-TNRs layer, r-TNRs/r-TNFs bilayer and anatase-phased TiO₂ as a photoelectrode

CHAPTER 1

Introduction and background of research

1.1 Introduction

The need for alternative energy sources is ever more pressing and demanding. Fossil fuel reserves are becoming scarce, making their exploration ever more expensive than ever. There are also the sensitive geopolitical issues in many parts of the world with the largest fossil fuel reserves. The more important is the reports from entities such as increase in green-house gases and the accelerated changes observed in climate, e.g. global warming. The alternatives are as geothermal, tidal, water cycle, atmospheric movements and solar radiation. All these are consequence of the earth's inherent heat, gravitational perturbations by the moon and sun, and solar radiation. The most abundant and equally distributed of these sources is probably solar radiation. In one hour the Sun delivers the same amount of energy consumed by the whole of humanity in one year. The photovoltaic (PV) effect whereby electricity can be generated via absorption of light is an attractive mean of directly generating electrical power.

1.2 Solar cell history

1.2.1 Early stage of solar cell

The most popular approach is based on silicon p-n semiconductor junction cells first demonstrated at Bells Labs in 1954 by Chaplin, Fuller and Pearson [1]. In the past 30 years, the cost of them has dropped by a factor of 20 with efficiencies reaching 18% for commercially available modules. For this type of device the theoretical limit (Shockley-Queisser limit) is 31%

[2]. Overall, this means that although the silicon-based cells have not reached their limit, there is only a 50% gain to be obtained. Thus, the main area of interest with silicon based PV modules lies in making them more economically viable by cheaper manufacturing and increasing their working lifetime. Currently the production of electricity via PV is still an order of magnitude more expensive than by e.g. gas, \$0.30 per kWh versus \$0.03 per kWh respectively [3].

Silicon based solar cells are the holders of the market, breaking down into three categories; single crystal, polycrystalline and amorphous. Due to the high-energy requirements involved in purifying silicon, the cost can be prohibitive due to the long payback time (10 to 20 years). There are, however, niches for each type of structure. Polycrystalline silicon although less efficient, is also used due to reduced manufacturing costs. These cells though are fraught with lower efficiencies due to the recombination properties of the grain boundaries. The determining factors for cost are not only crystal growth. These cells need to be packaged and positioned, both of which have costs associated with them. Group III/IV direct band gap semiconductor materials are also utilized in cases where efficiency is a prime objective over cost, such as the space industry. Whereas a thickness of 100 μm is required for 90% absorption in silicon, only 1 μm in GaAs is required for the same absorption. The main reason for this is that GaAs is a direct band gap semiconductor and thus excitation of an electron does not require the aid of a phonon for momentum transfer. There are also efforts into making ribbon silicon [4]. Again, the aim is the reduction of manufacturing costs, this time by circumventing the sawing of crystal ingots (40% waste). Investigation has gone into over a score of different approaches in manufacturing ribbon silicon with some already in the pilot scheme state [5]. Impressively, these types of cells demonstrate up to 15% efficiencies and with silicon production yields up to 90%.

1.2.2 Middle stage of solar cell

Second generation solar cells [6] appeared in the 1970's. There are mainly two variants; copper indium diselenide [7] and cadmium telluride [8] both coupled with n-type cadmium selenide (CdS) to create p-n heterojunction. Due to the large band gap of CdS (2.4eV), it is utilised as a window to the p-n junctions. As direct band gap semiconductors, only a thin film (10 μm in thickness) is required for complete light absorption unlike to first generation silicon cells (100 μm in thickness). Even though laboratory results for CuInSe_2 cells have been promising, there is still the need for a complete understanding of these ternary compound semiconductors. In addition, because they are ternary, the manufacturing techniques required are complex especially on the up scaling. Furthermore, there is debate as to the validity of using rare elements such as indium. On the other hand, CdTe has an excellent solar matching absorption spectrum with a band gap of 1.5 eV and is relatively easy to handle as a thin film. This implies that photons of energy above 1.5 eV will be absorbed and converted to electrons, and at 1.5 eV this is a large proportion of the solar spectrum. However, due to large differences in work functions with the metals used for contacting, there are problems in creating low resistance ohmic contacts. In addition, the toxicity of the materials has been an environmental concern.

1.2.3 Current stage of solar cell

The term describing third generation solar cells is mostly used to describe systems which do not fall into the first or second generations and/or that try to circumvent the 31% Shockley-Queisser limit. This can be achieved by e.g. concentrating the light source [9], use of tandem cells with multiple band gaps [10] or conversion of photons [11], where more than one electron-hole pair are generated per photon. These systems are costly and complex to prepare. However,

there are also the third generation cheaper alternatives. These can be split into two categories, the organic heterojunctions [12] and dye-sensitized solar cells [13].

The dye-sensitized solar cell (DSC) also commonly known as the Grätzel cell [13] is another alternative which has attracted much attention. Large volume of published work is a consequence not only of the need for alternative forms of energy but also the large variety of physical and chemical processes that govern a DSC. It is somewhat intriguing that a DSC being relatively simple and cheap to manufacture, (e.g. no need for clean room facilities compared to more classical photovoltaic system) is still today without a coherent model describing its photovoltaic properties. The current record efficiency for the DSC in optimised laboratory conditions stands at 11.1% [14].

1.3 Structure of Dye-Sensitized Solar Cells (DSC)

The DSC consists of five different components; first component is a transparent conductive oxide (TCO) being used as the front electrode, second is an n-type semiconductor TiO_2 thin film, third is a dye-sensitizer, fourth is an electrolyte and fifth component is a platinum coated glass as the counter electrode. Figure 1.1 illustrates the diagram of conventional DSC. Every component has its function to perform for the DSC.

a. Transparent conductive oxide (TCO) layer

TCO layer works as a conductive electrode which is used to connect from DSC to outer circuit to complete the circuit of DSC.

b. n-type semiconductor nanocrystalline TiO_2 thin film

Nanostructured TiO_2 thin film which acts as a photoelectrode has two functions in DSC:

- a) It provides the surface for the dye adsorption
- b) It functions as electron acceptor for the excited dye and it serves as electron conductor.

c. Dye-sensitizer

Dye is a photoactive element of the photovoltaic device, harvesting the incident light for the photon-to-electron conversion. The dye should ideally cover a wide range of the solar spectrum. More than 50 % of the solar energy is emitted in the region from 400 to 800 nm.

d. Electrolyte

A medium for regenerates the oxidised dye molecule.

e. Platinum coated glass as counter electrode

The counter electrode has ideally a high conductivity and been used to complete the circulation operation of DSC.

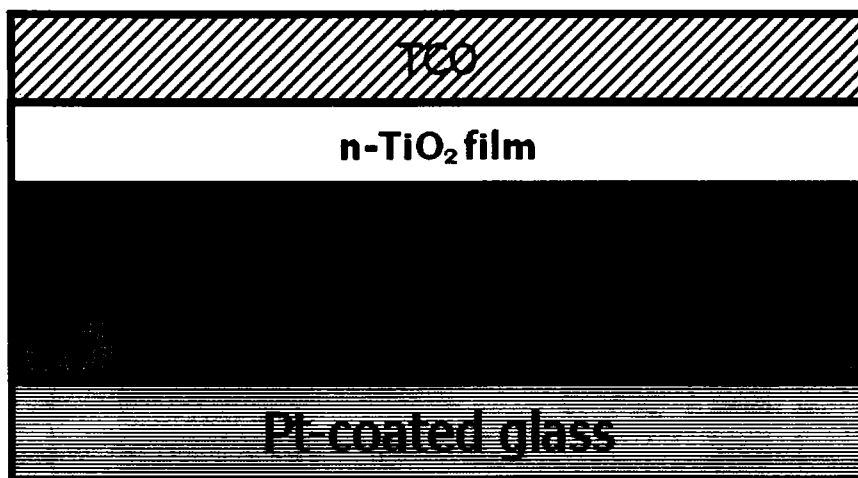


Figure 1.1 Configuration of conventional Dye-sensitized Solar Cell (DSC)

The dye-sensitized solar cell is composed of two surfaces of highly transparent conductor material mostly from conducting oxide on glass. On top of the conductor material, there is a few micrometer thick film of wide band gap semiconductor which is formed of a self connected network, highly surface area and porosity with nanometer size particles. The energy conversion in the DSC is based on the injection of an electron from a photoexcited state of the sensitizer dye into the conduction band of the nanocrystalline semiconductor, as illustrated in Figure 1.2 [15]. The solar cell employs a liquid electrolyte, usually an iodide or triiodide redox active couple dissolved in an organic solvent which is to reduce the dye cation (regenerate the ground state of the dye).

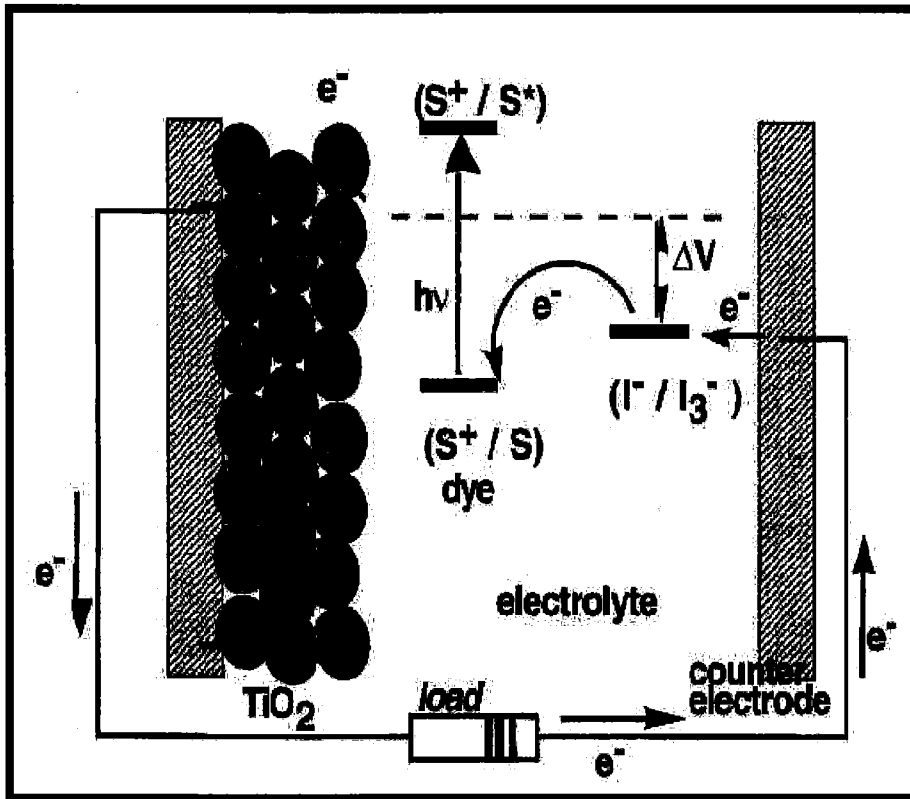


Figure 1.2 Principle operation of Dye-Sensitized Solar Cell (DSC) [15]

Dye-sensitized solar cell is a device for the conversion of visible light into electricity based on the sensitization of wide band gap semiconductor. The TiO_2 is a transparent semiconductor material which has melting and boiling points of 1870°C and 2972°C , respectively [16]. TiO_2 is material with excellent merits in solar energy transferring and photo-catalysis of poison compounds in environment [17]. As a semiconductor material, TiO_2 has indirect band gap and n-type semiconductor which has band gap energy of 3.2 eV at room temperature [18].

1.4 Hydrothermal method

1.4.1 History and definition of hydrothermal method

The term hydrothermal is purely of geological origin. It was first used by the British Geologist, Sir Roderick Murchison (1792-1871) to describe the action of water at elevated temperature and pressure in bringing about changes in the earth's crust leading to the formation of various rocks and minerals [19]. An understanding of the mineral formation in nature under elevated pressure and temperature conditions in the presence of water led to the development of the hydrothermal technique. It was successfully adopted by Schafthaul (1845) to obtain quartz crystals upon transformation of freshly precipitated silicic acid in Papin's digester [20].

The first successful commercial application of hydrothermal technology began with mineral extraction or ore beneficiation in the previous century. The use of sodium hydroxide to leach bauxite was invented in 1892 by Karl Josef Bayer (1871-1908) as a process for obtaining pure aluminium hydroxide which can be converted to pure Al_2O_3 suitable for processing to metal [21]. The principle involved is quite simple, very effective, and inexpensive as shown below, for example.



The above process is easy to achieve and the leaching can be carried out in a few minutes at about 330°C and 25,000 kPa [22].

According to Laudise (1970), hydrothermal growth means growth from aqueous solution at ambient or near-ambient conditions [23]. Rabenau (1985) defined hydrothermal synthesis as the heterogeneous reactions in aqueous media above 100°C and 1 bar [24]. Roy (1994) declares that

hydrothermal synthesis involves water as a catalyst and occasionally as a component of solid phases in the synthesis at elevated temperature ($>100^{\circ}\text{C}$) and pressure (greater than a few atmospheres) [25]. Byrappa (1992) defines hydrothermal synthesis as any heterogeneous reaction in an aqueous media carried out above room temperature and at pressure greater than 1 atm [26]. Yoshimura (1994) proposed the following definition: reactions occurring under the conditions of high-temperature-high-pressure ($>100^{\circ}\text{C}$, >1 atm) in aqueous solutions in a closed system [27].

All definitions mentioned above hold good for materials synthesis, metal leaching and treatment of waste materials. From all researchers mentioned above show that hydrothermal method is one of the best methods for materials synthesis at low temperature with high pressure in a closed system.

1.5 Background research

1.5.1 Dye-sensitized solar cell

Dye-sensitized solar cell (DSC) is conventionally based on anatase TiO_2 as photoelectrode. Recently, Yella et al. and co-workers [28] studied and they prepared cobalt (II/III) based electrolyte to increase the wavelength for porphyrin dye to absorb more light. They managed to get 12.3% of power conversion efficiency. For other study, Xin et al. [29] shows that the efficiency of DSC was increased when the surface of TiO_2 was treated by measured different thickness. In this study, the TiO_2 thickness of 20 μm is the optimum thickness to give the highest efficiency.

All of these DSCs usually consist of a mesoporous anode formed by a sintered film of anatase TiO_2 which serves as the electron acceptor and a transport layer coated with a thin layer of sensitizer dye molecules for light absorption and electron injection into the TiO_2 conduction band. A liquid electrolyte generally consists of an organic solvent such as acetonitrile and a redox couple I^-/I_3^- that serves as a redox agent to reduce the photoexcited dye molecules. Preparation of TiO_2 film affects the pore size distribution, porosity, and crystallinity and then all of these correlate with the transport of electrons and diffusion of electrolyte in the cells. There are many efforts focusing on improving this system by altering the particle size and morphology of TiO_2 optimizing the fabrication and structure of the TiO_2 film, developing new sensitizers, suppressing charge recombination, and improving interfacial energetics.

1.5.2 Advantages of one dimensional nanostructured rutile-phased TiO_2 towards DSC

High performance DSC requires nanoscale and highly crystalline TiO_2 electrode with large surface area and favourable electrical contiguity with conducting glass substrate so that dye molecules can be sufficiently adsorbed and electrons can be quickly transferred. According to above concept, TiO_2 film electrodes with 1-dimensional nanoparticle size could give high surface areas for better efficiency. It is known in the realm of nanoscience and nanotechnology that nanorods, nanowires and nanotubes play special roles because of their one dimensionality. When the diameter of the nanorods, nanowires and nanotubes become small, the physico-chemical properties of the one-dimensional nanostructure are clearly different from those of crystalline solids or even two-dimensional system. DSCs are rather complicated system including such processes in a series as light absorption, charge injection, charge collection and electrolyte diffusion. They are many factors that influence the result in light to electricity

conversion efficiency of DSCs. One of the factors is the electron transport in the mesoporous TiO₂ film. Surface state of the particles, the channel and connection between particles and the morphology are the things that change many electrical and physical properties of DSC. The use of one-dimensional TiO₂ films is one of the most promising routes to higher efficiency, because the barrier effect of intercrystalline TiO₂ is greatly decreased by long crystalline one-dimensional TiO₂ film. Inspiringly, Grimes and Aydil have synthesized single crystalline TiO₂ nanowires and nanorods on FTO (fluorine doped tin dioxide) by a facile hydrothermal method. [30-31]. But this novel nanostructure may have a low amount of dye adsorption and light harvesting efficiency because of the large number of gaps existing among the nanorods.

1.5.3 Rutile based dye-sensitized solar cell and its advantages

Rutile TiO₂ is thermodynamically stable obtained via phase transition from anatase to rutile, which requires a high temperature sinter process. Rutile phase TiO₂ is the most commonly used white pigment in paints. It is favoured over anatase for this purpose because the rutile scatters white light more efficiently and is chemically stable. Recently, a study on the rutile based DSC has been performed and revealed that the photovoltaic characteristics at one sun light intensity are comparable to those of conventional anatase TiO₂ based solar cell.

The comparison of anatase based DSC and rutile-based DSC has already done by Park and et al [32]. In their study, rutile based DSC has insufficient dye adsorption compared to anatase based DSC. From this, modification towards enhancement in dye adsorption in rutile based DSC could increase the performance of rutile based DSC. Treelike TiO₂ nano-arrays grown on metal titanium foils were prepared by Wu and co-workers, but their application in DSC is limited due to the foils were non transparent [33]. Park and co-workers used rutile TiO₂ branched

nanostructures synthesized by the seeding method for dye-sensitized solar cells, but the one-dimensional nanostructures still lay in the plane of the FTO [34].

From the background studies, the performance of rutile based DSC can be increased if good dye adsorption and better electron transportation are realized.

1.6 Thesis objectives

The main aim of the research is to prepare one-dimensional rutile phased nanostructured TiO_2 film for dye-sensitized solar cell. Hydrothermal method was used in the preparation of rutile TiO_2 film due to low cost, simple process, and the sample can be prepared at low temperature. The four main procedures of this project are:

- i. To prepare rutile phased nanostructured TiO_2 film using hydrothermal method.
- ii. To apply rutile phased nanostructured TiO_2 film in DSC application.
- iii. To increase performance of rutile based DSC using rutile phased TiO_2 nanostructures prepared.

From all of the mentioned procedures, rutile nanostructure TiO_2 films have been prepared and the performance of DSC has been measured. As a consequence one-dimensional nanostructure rutile based TiO_2 film has enhanced the performance of DSC.

1.7 References

- [1] D.M. Chapin, C.S. Fuller and G.L. Pearson, *Journal of Applied Physics*, 25 (1954) 676.
- [2] W. Shockley and H.J. Queisser, *Journal of Applied Physics*, 32 (1961) 510.
- [3] E. Cartlidge, Bright outlook for solar cells, in *Physics World*. (2007).
- [4] M.A. Green, *Solar Energy*, 74 (2003) 181.
- [5] W. Schmidt, B. Woesten and J.P. Kalejs, *Progress in Photovoltaics*, 10 (2002) 129.
- [6] R.W. Birkmire and E. Eser, *Annual Review of Materials Science*, 27 (1997) 625.
- [7] L.L. Kazmerski, F.R. White and G.K. Morgan, *Applied Physics Letters*, 29 (1976) 268.
- [8] D.A. Cusano, *Solid-State Electronics*, 6 (1963) 217.
- [9] R.R. King, D.C. Law, K.M. Edmondson, C.M. Fetzer, G.S. Kinsey, H. Yoon, R.A. Sherif and N.H. Karam, *Applied Physics Letters*, 90 (2007) 18.
- [10] V.M. Lantratov, N.A. Kalyuzhnyi, S.A. Mintairov, N.K. Timoshina, M.Z. Shvarts and V.M. Andreev, *Semiconductors*, 41 (2007) 727.
- [11] A. Luque, A. Marti and A.J. Nozik, *Mrs Bulletin*, 32 (2007) 236.
- [12] T.L. Benanti and D. Venkataraman, *Photosynthesis Research*, 87 (2006) 73.
- [13] B. O'Regan and M. Grätzel, *Nature*, 353 (1991) 737.
- [14] Y. Chiba, A. Islam, Y. Watanabe, R. Komiya, N. Koide and L.Y. Han, *Japanese Journal of Applied Physics Part 2-Letters & Express Letters*, 45 (2006) 638.
- [15] M. Gratzel, *Prog. Photovolt. Res.*, 8 (2000) 171.

- [16] R. J. C. Brown and R. F. C. Brown, *Journal of Chemical Education* 77 (2000) 724.
- [17] M.R. Hoffmann, S.T. Martin, W. Choi and D.W. Bahnemann, *Chem. Rev.*, 95 (1995) 69.
- [18] Y.W. Wang, L.D. Zhang, G.Z. Wang, X.S. Peng, Z.Q. Chu and C.H. Liang *Journal of Crystal Growth* 234 (2002), 171
- [19] Sir Roderick Murchison (1840)
- [20] Schafthaul, K. F. E., *Gelehrte Anzeigen Bayer. Akad.*, 20 (1845) 592.
- [21] Goranson, R. W., *Journal of Science* 21 (1931) 481.
- [22] Habashi, F. *Proceeding First International Conference Solvothermal Reactions* (1993)
- [23] Laudise, R. A. *The Growth of Single Crystals* (1970) 278.
- [24] Rabenau, A., *Angew. Chem.* 24 (1985) 1046.
- [25] Roy, R., *J. Solid State Chem.*, 111 (1994) 11.
- [26] Byrappa, K. *Hydrothermal Growth of Crystals Pergamon Press* (1992) 1.
- [27] Yoshimura, M. and Suda, H., *Hydroxyapatite and Related Materials* (1994) 45.
- [28] Yella, A., Lee, H. -W, Tsao, H. N., Yi, C., Chandiran, A. K., Nazeeruddin, Md. K., Diau, E. W.-G., Yeh, C. -Y, Zakeeruddin, S. M., and Gratzel, M., *Science* 334 (2011) 629.
- [29] Xin, X., Scheiner, M., Ye, M., and Lin, Z., *Langmuir* 27 (2011) 14594.
- [30] Feng, X. j., Shankar, K., Varghese, O. K., Paulose, M., Latempa, T. J., and Grimes, C. A., *Nano Letter* 8 (2008) 3781.
- [31] Liu, B., and Aydil, E. S., *J. Am. Chem Soc.*, 131 (2009) 3985.

- [32] Park, N. -G., Van de Langemaat, J., and Frank, A. J., *J. Phys. Chem B* 104 (2000) 8989.
- [33] Yang, X. F., Zhuang, J., Li, X. Y., Chen, D. H., Ouyang, G. F., Mao, Z. Q., Han, X. Y., He, Z. H., Liang, C. L., Wu, M. M., and Yu, J. C., *ACS Nano* 3 2009 1212.
- [34] Oh, J. K., Lee, J. K., Kim, H. S., Han, S. B., and Park, K. W., *Chem Mater.*, 22 2010 1114.

CHAPTER 2

Growth and application of TiO₂ nanorods in DSC using hydrothermal method

2.1 Introduction

Dye-sensitized solar cells (DSCs) developed by Grätzel and co-workers are attracting widespread academic and industrial intense interest due to their high solar conversion efficiency over 10% at a very low cost of production [1–3]. Recently, many researcher and scientist groups have focused on relevant studies to attempt to use different nanomaterials such as nanotubes, nanopillars, nanoleaves, nanoflowers and nanospheres in the DSC applications. There are many ways to prepare the nanomaterials such as electron beam evaporation [4], ion sputtering [5], chemical vapour deposition [6], and hydrothermal method [7]. Nowadays, the hydrothermal process has been successfully used for the TiO₂ nanomaterials due to its low cost and highly stable process and uniformed resultant film. In this study, we have successfully prepared TiO₂ nanorods for film with different precursor concentrations using the hydrothermal method. All nanorods based TiO₂ thin films were then used in the DSC application. We also studied surface morphologies and structural properties of the films prepared with different precursor concentrations and their relations with the DSC application.

2.2 Experimental

The FTO (fluorine doped tin dioxide) coated glass was used as a substrate. The substrates were cleaned with acetone, ethanol and deionised water (DI water) using 1:1:1 volume ratio and finally cleaned using ultrasonic method for 1 h.

Hydrothermal process done in the present experiment was using chemical solutions which are mixing of concentrated hydrochloric acid (HCl) as chelating agent, titanium butoxide (TBOT)

and DI water for the hydrolysis process. 20 ml of HCl and 20 ml of DI water were mixed and stirred at ambient condition for about 5 min. The mixture was continually stirred after adding 0.5 ml, 0.7 ml and 1.0 ml of TBOT for about 5 min. Cleaned FTO coated glass was put into teflon-lined steel, autoclave (50 ml volume) with conducting side of the FTO facing upward. The hydrothermal process was done at 150 °C for 20 h. The autoclave was then cooled to room temperature for about 20 min. The substrate was taken out and rinsed with DI water and dried in ambient air.

Electrolyte was prepared using 0.6 M of 1,2-dimethyl-3-propylimidazolium iodide, 0.1 M LiI, 0.5 M of 4-tert-butylpyridine, 0.1 M of guanidine thiocyanate, 0.85 ml of acetonitrile, 0.5 ml of valeronitrile and 0.05 M of I₂.

Dye solution was prepared at 3 mM which contained acetonitrile, butyl alcohol and ruthenium dye (N719). The samples were immersed into dye solution for about 14 h.

DSC fabrication was done by using FTO coated and Pt coated glasses as a front electrode and a counter electrode, respectively. The TiO₂ nanorods film with electrolyte was covered with the counter electrode to complete the solar cell configuration. Crocodile clip was used to clamp both electrodes for I-V measurement.

The surface morphology of samples were observed using field-emission scanning electron microscopy (FE-SEM) (JSM-6320F), the crystallinity of samples was analyzed with thin film X-Ray Diffraction (XRD) (RINT Ultima III) and I-V measurement was measured using solar simulator under 1.5 AM (Bunkoh Keiki-JUSCO).

2.3 Results and Discussion

2.3.1 Surface morphology

Surface morphology of the film cross sections was analyzed using FE-SEM and the images of TiO₂ nanorods (TNRs) films prepared using 0.5 ml, 0.7 ml and 1.0 ml of TBOT are shown in Figures 2.1, 2.2 and 2.3, respectively.

It is indicated from Figure 2.1(a) that at 0.5 ml of TBOT, vertically oriented TNRs together with some mis-oriented nanorods were obtained and only few TiO₂ nanoflowers (TNFs) can be seen on the surface. The gaps among TNRs are about 0.5 μm and there are 3 to 4 μm -sized holes on the TNRs film. At 0.7 ml of TBOT, there are TNFs deposited on top of TNRs film as shown in Figure 2.2(a). The diameter of nanorods that compose the TNFs is about 1 μm . There are also cracks on the film, and the holes were less compared with Figure 2.1(a). Many TNFs are observed at 1.0 ml of TBOT as shown in Figure 2.3(a). The size of nanorods for the TNFs is about 1 μm , which is same as that in Figure 2.2(a). The TNFs are more uniformly deposited on top of the TNRs film compared with Figure 2.2(b).

The thickness of all films is about 10 μm as revealed from Figure 2.1(b) to Figure 2.3(b). It is also suggested that the gap among TNRs is decreased when the TBOT concentration is increased.

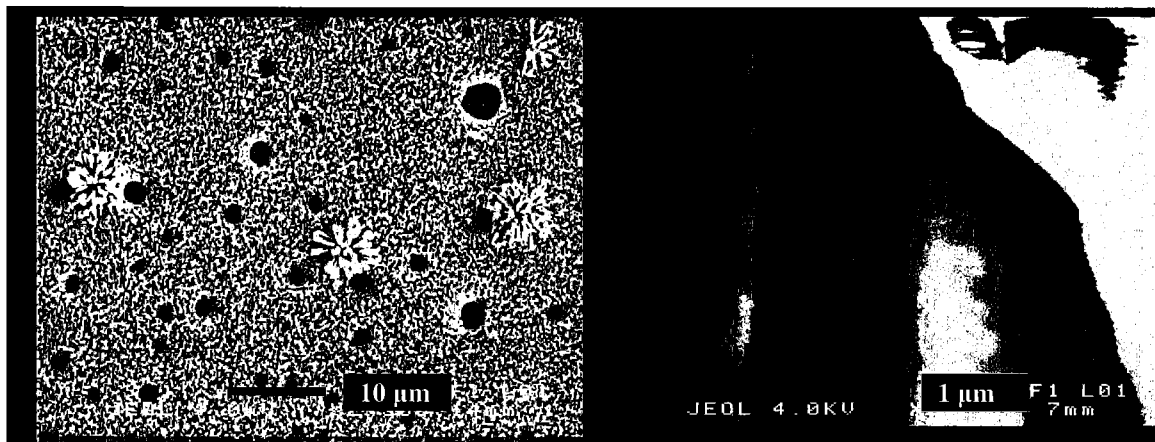


Figure 2.1 (a) the surface morphology of nanostructured TiO_2 film synthesized at 150°C with 0.5 ml of TiO_2 precursor and (b) its cross section

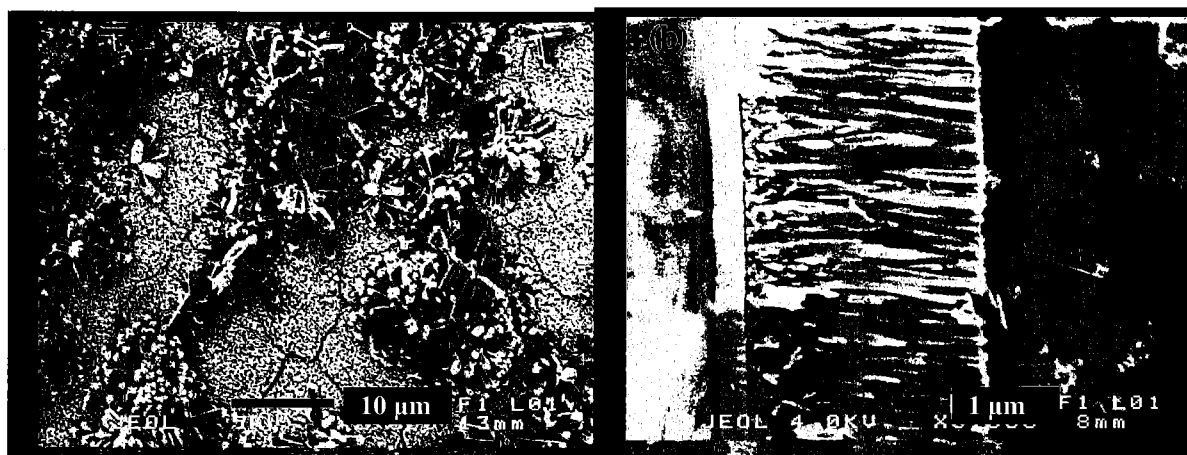


Figure 2.2 (a) the surface morphology of nanostructured TiO_2 film synthesized at 150°C with 0.7 ml of TiO_2 precursor and (b) its cross section

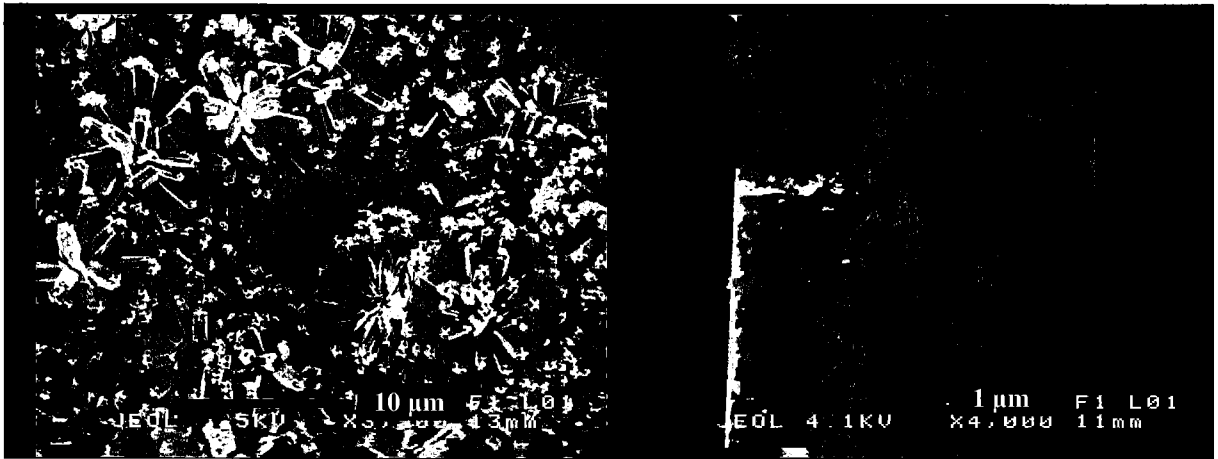


Figure 2.3 (a) the surface morphology of nanostructured TiO₂ film synthesized at 150°C with 1.0 ml of TiO₂ precursor and (b) its cross section

2.3.2 Structural property

The structural properties of TiO₂ thin film were carried out with Cu-K α radiation and 2° grazing angle. Figure 2.4 shows XRD profiles of the TNRs films which were prepared at different concentrations of TBOT. The XRD profiles show that both the TNRs film prepared with 0.5 ml and 0.7 ml have two kinds of crystallinity phases, anatase and rutile phases. The reason for the anatase phase is still in investigation. It might be related to a completeness of the crystallinity. The anatase phase is completely disappeared when the TBOT concentration is increased to 1.0 ml. The highest crystallinity of TNRs film is shown in Figure 2.4(c). Three main peaks at 27.42°, 36.04° and 41.20° correspond to the rutile [110], [101] and [111] crystal planes, respectively. The results agree with those obtained by T.-D Nguyen Phan et al. [8]. All the rutile peaks observed are confirmed by PDF No. 98-000-0090 and the anatase peaks by PDF No. 98-000-0008.

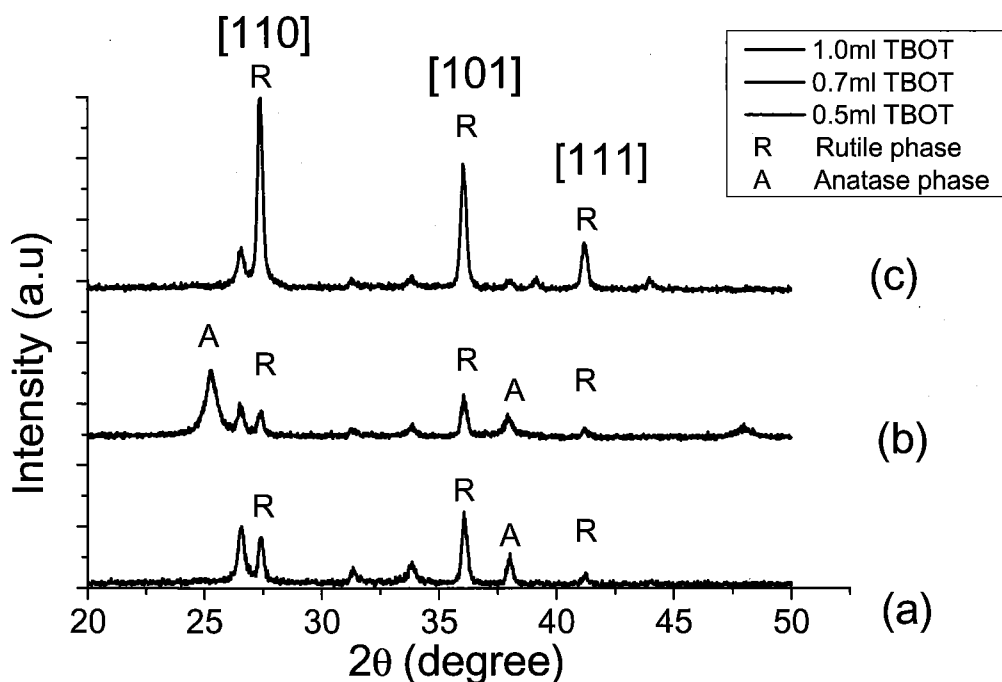


Figure 2.4 XRD profiles of TNRs film with different TBOT concentrations; (a) 0.5ml, (b) 0.7ml and (c) 1.0ml

2.3.3 Photovoltaic properties

Figure 2.5 shows the I-V characteristics of DSC composed of FTO/TNRs+dye+electrolyte/Pt, and the photovoltaic properties are summarized in Table 2.1, where J_{sc} is a short circuit current density, V_{oc} is an open circuit voltage and η is energy conversion efficiency. It is confirmed that the DSC based on the TNRs film with 1.0 ml of TBOT gives the highest efficiency, and that the efficiency is increased as the precursor concentration is increased. The increase in efficiency is mainly due to an increase in J_{sc} , which indicates an increase in the dye adsorption of TNRs film. The dye adsorption is closely related to the surface morphology of film itself. As the concentration of TBOT increases, the density of TNFs increases as shown in Figures 2.1, 2.2 and 2.3. The increased TNFs might increase a surface area of the film and thus give a higher dye

adsorption. Although the efficiency of 0.40% is much lower compared to other researchers [9], increase in the thickness and control of the TNFs growth could enhance the dye adsorption and photovoltaic properties, and finally increase the DSC efficiency.

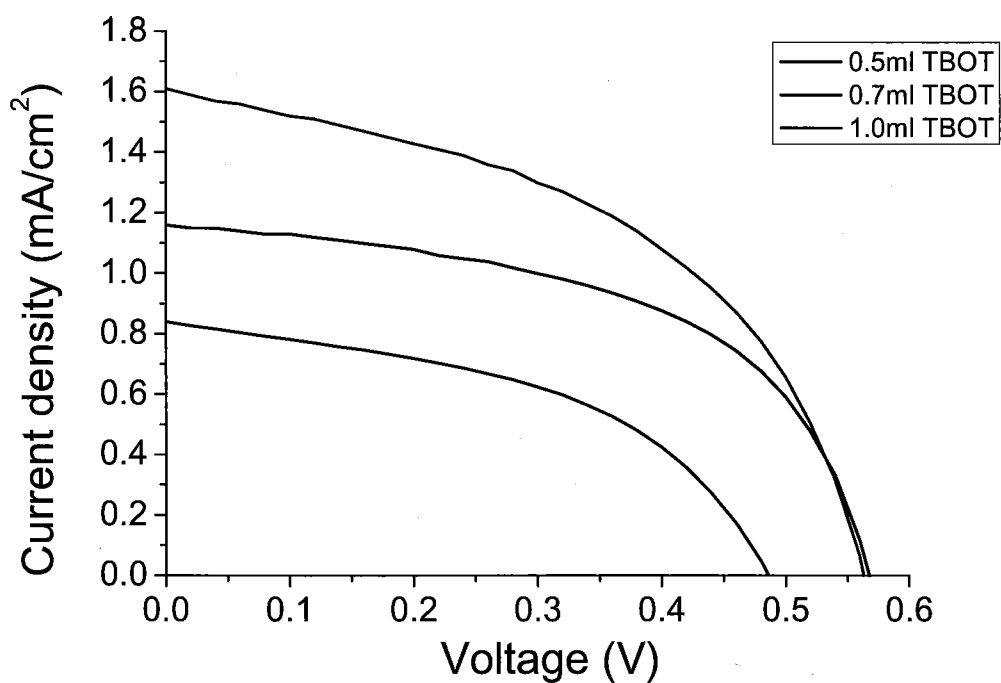


Figure 2.5 I-V characteristics of DSC based on the TNRs films with different TBOT concentrations

Table 2.1

Photovoltaic properties of DSC with different TBOT concentrations

TBOT content (ml)	Jsc (mAcm ⁻²)	Voc (V)	Fill factor	η (%)
0.5	0.838	0.486	0.471	0.192
0.7	1.161	0.568	0.535	0.353
1.0	1.610	0.563	0.477	0.432

2.4 Conclusion

The TiO₂ nanorods have been successfully deposited onto the FTO coated glass substrate using a hydrothermal method. The DSC was also successfully fabricated without post-annealing process. From the SEM images, the thickness of TNRs and amount of TNFs are increased when the amount of precursor is increased. XRD pattern suggested that, all peaks at 0.5 ml and 1.0 ml of TBOT are corresponded to rutile phase. Only at 0.7 ml of TBOT gives anatase peaks. This is due to experimental errors and the transformation from rutile phased to anatase phase in this study is not suggested.

It is confirmed that the DSC based on the TNRs film with 1.0 ml of TBOT gives the highest efficiency, and that the efficiency is increased as the precursor concentration is increased. The increase in efficiency is mainly due to an increase in Jsc, which indicates an increase in the dye adsorption of TNRs film. The dye adsorption is closely related to the surface morphology of film itself. As the concentration of TBOT increases, the density of TNFs increases as shown in Figures 2.1, 2.2 and 2.3. The increased TNFs might increase a surface area of the film and thus give a higher dye adsorption. Although the efficiency of 0.40% is much lower compared to other

researchers [9], increase in the thickness and control of the TNFs growth could enhance the dye adsorption and photovoltaic properties, and finally increase the DSC efficiency.

2.5 References

- [1] B. O'Regant, M. Gratzel: *Nature* 353 (1991) 737.
- [2] M. Gratzel: *Nature* 414 (2001) 338.
- [3] M. Gratzel: *J. Photochem. Photobiol. A: Chem*, 164 (2004) 3.
- [4] Y.L. Wang, K.Y. Zhang: *Surf. Coat. Technol.* 140 (2001) 155.
- [5] S. Takeda, S. Suzuki, H. Odaka, H. Hosono: *Thin Solid Films* 392 (2001) 338.
- [6] H.Y. Ha, S.W. Nam, T.H. Lim, I.H. Oh, S.A. Hong: *J. Membr. Sci.* 111 (1996), 81.
- [7] Y. Xiao, J. Wu, G. Yue, G. Xie, J. Lin and M. Huang: *Electrochimica Acta* 55 (2010), 4573.
- [8] T.-D Nguyen Phan, H.-D Pham, T.V. Cuong, E.J. Kim, S. Kim and E.W. Shin: *Journal of Crystal Growth* 312 (2009), 79.
- [9] H. Kyung-Jun, S. Wang-Geun, J. Sung-Hoon, Y. Seung-Joon and L. Jae-Wook: *Appl. Surf. Sci.* 256 (2010), 5428.